The Applicability of Statnamic Load Test for Micropile

Yasumitsu Ichimura[1]
Takeshi Oshita[1]

[1]Public Works Research Institute,Ministry of Construction

ABSTRACT

In Japan, high capacity micropiles reinforced with steel pipe are expected to be an effective method of meeting the growing need to reinforce damaged foundations and perform seismic retrofitting of existing foundations that has appeared since the Hyogo-ken Nanbu Earthquake of 1995. The use of high capacity micropiles for seismic retrofitting has been spreading in the United States in recent years, but it has not been done in Japan. To prepare for its use here, full-scale piles were constructed and used for static load testing and Statnamic load testing in order to clarify vertical bearing capacity of micropiles.

1.INTRODUCTION

The need for seismic retrofitting of existing structures has grown since the Hyogo-ken Nanbu Earthquake. Bridge piers are being reinforced with steel plates, but it is also essential to reinforce the foundation under the bridge footings in order to increase the seismic resistance of overall structural systems. But in urban areas, there are cases where conditions at these sites make it difficult to bring in large construction machinery and others where increasing the number of piles or improving the ground are impossible because of restrictions on headroom. Micropile work is a construction method that can be applied widely to the reinforcement of existing structures because it is done by boring holes in the ground with small boring machines then injecting grout to form each micropile. For this reason, in the United States, the use of micropiles for the seismic retrofitting of existing structures has been done with increasing frequency in recent years, but here in Japan, the use of micropiles for this purpose is still rare.

To guarantee that micropiles provide the necessary bearing capacity, it is important to practice appropriate execution control and quality control. It is also vital to carry out load testing to directly confirm the bearing capacity of a number of piles at a site. Static load testing is the common way to find the bearing capacity of a pile, but because this is a time consuming and expensive process, it is difficult to do at a site. For this reason, a way must be found to increase the number of piles tested using a simpler and lower cost method. Statnamic load testing is a method that meets such needs.

For the above reasons, full-scale test piles were constructed and used for vertical load testing in order to clarify vertical bearing capacity of micropiles reinforced with steel pipes. This report compares the results of Statnamic load testing with the results of static load testing of micropiles in order to judge the applicability of the Statnamic load testing. It also reports on the execution of integrity testing that is a non-destructive pile length and shape estimation method.

2.OUTLINE OF FIELD TEST

(1) Test piles and ground conditions

Table 1 shows the specifications of the test piles. Two test piles called pile A and pile B were made with the distance between their center points of 3.0 m. The only difference between them was the bond length of the grout (Pile A: 5.18 m, Pile B: 1.01 m). Figure 1 shows the ground conditions at the site, the penetration length of the pile, and the locations of the sensors. The ground is a

Table 1. Test Pile Specifications

Material Constituents	Specifications
Seamless Steel Pipe for Oil Well Work	Outer diameter: 177.8 mm Wall thickness: 12.7 mm
Threaded Deformed Bars	SD345 D51 Length (pile length): 21.85 m (pile A) 17.68 m (pile B)
Grout (High Early Strength Cement, Water)	Water/cement ratio: 45% Compressive strength: 35 N/mm^2 Tip diameter: 254 mm Bond length: 5.18 m (pile A) 1.01 m (pile B)

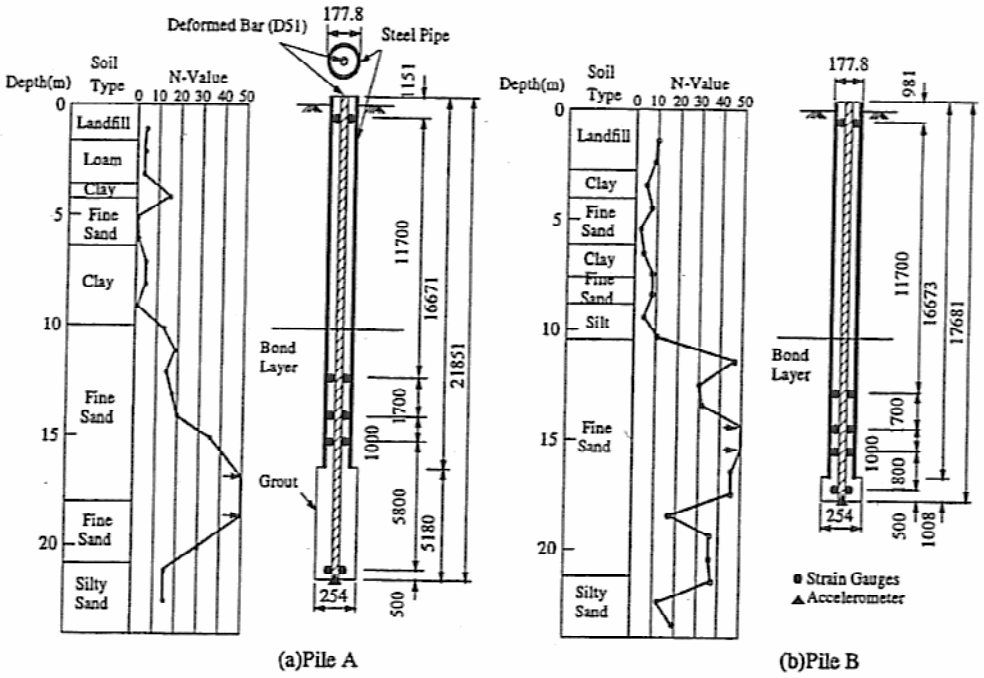

Figure 1. Ground Conditions and Sensor Locations at the Test Site

fine sand layer below GL−10 m. Near GL−17 m in the grout bond length, there is a sand layer containing gravel with an N-value greater than 40.

(2) Test pile construction method

The micropiles were constructed at the site as shown in Figure 2. First, with the steel pipe used as reinforcing material serving as a casing, a bore hole was formed with a small boring machine, next a deformed reinforcing steel bar was inserted, and finally grout was injected (primary injection). Next the casing was withdrawn to a specified level and grout was injected under pressure (secondary injection). The grout was injected at a pressure of 0.5 Mpa.

(3) Load test conditions

Figure 3 shows the testing procedure. The static load testing was done on both pile A and Pile B 1 month after they were constructed. Then the Statnamic load testing of pile A was performed 2 weeks after the static load testing. The planned load for the Statnamic load testing was set at 2 MN (reaction mass 20 tons, propellant; 1.7kg) and the test was done using an 8 MN loading device that is the smallest in use in Japan. After the load testing was completed, an integrity test was performed. The integrity test was performed by installing an accelerometer on the grout at the top of the pile and striking the

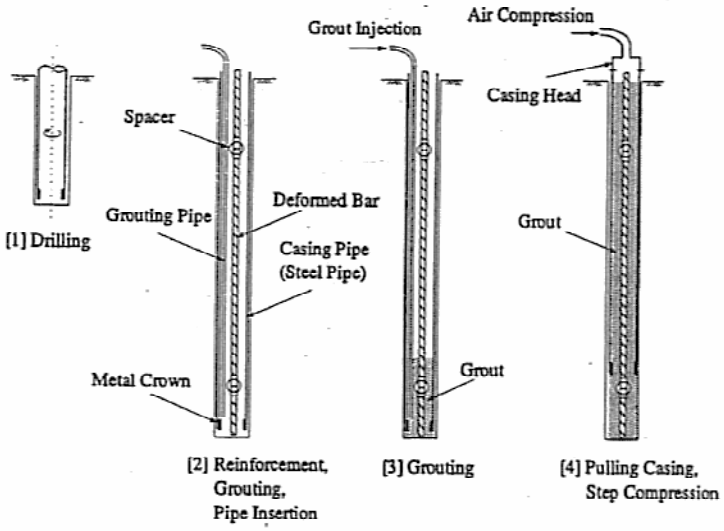

Figure 2. Micropile Construction Method

pile lightly with a plastic hammer.

3. FIELD TEST RESULTS

(1) Bearing capacity of micropile (Static load test results)

Figure 4 shows the load – displacement curves of pile A and pile B obtained from the static load testing. As a result of judgments based on this figure and on other curves (logP – logS curve, etc.), the first and second limit loads of pile A and of pile B are as shown in Table 2. This demonstrates that pile A has between 1.6 times and 1.7 times the limit load of pile B, confirming that the grout bond length has a big effect on the limit load.

Figure 5 shows the axial force distribution of pile A. The figure reveals that the axial force of pile A is almost constant down to a depth of 12 m and that the skin friction of the steel pipe above the bond layer is extremely small. It also demonstrates that below a depth of 17 m on the grout bond section, the axial force drops abruptly and that in pile A, most of the bearing capacity is dependent on the skin friction of the grout and that the toe resistance is only a small percentage of this bearing capacity. Figure 6 shows the axial force distribution of pile B. The way that skin friction is generated on the grout on pile B is similar to that of pile A, but the skin friction of the steel pipe is much higher than that of pile A. This indicates that in Pile B, the grout circulated to a level far higher than the tip of the steel pipe. This is considered to be a result of the fact that the N-value is higher than 40 from a level close to GL–10 m in the ground at the location where pile B was installed shown in Figure 1 and that the ground conditions differ from those at the location where pile A was installed. This suggests that there are cases where it is possible to count on the support of skin friction not only in the grout section but, under certain ground conditions, in the steel pipe section as well.

Table 3 shows the results of finding the contributions of the skin friction and the toe resistance based on the above results. In pile A, the toe resistance accounted for 11% of the bearing capacity and in pile B, for about 18%. Because the grout bond section of pile B was smaller, the percentage contribution of the toe resistance was relatively higher. Table 4 shows a comparison of the skin friction of the grout section and the values specified in the standard of ground anchor. This table reveals that the values obtained from the load testing conform closely to standard values.

(2) Applicability of Statnamic load testing

As shown in Figure 7, Statnamic load testing involves thrusting a reaction mass upwards at an acceleration of about 20 G under the pressure of gas produced by the combustion of a propellant so that its reaction force acts on the top of a pile as a load. Because this method does not require a reaction pile or loading beam etc., it can be done at low cost in a short time, making it an effective way to confirm the bearing capacity of micropiles. But because the loading time is extremely short (about 0.1 second), the test results include dynamic effects, requiring correction to estimate the static resistance.

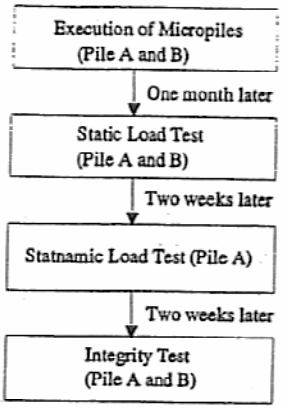

Figure 3. Test Procedure

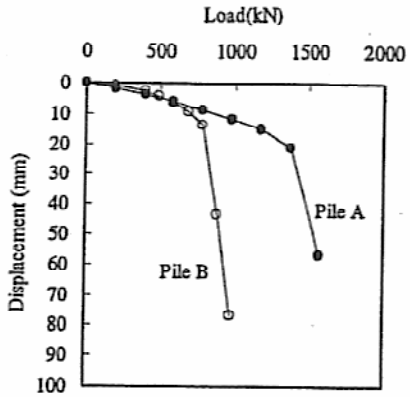

Figure 4. Load-displacement Curve (Static Load Test Result)

Table 2. The Limit Load Evaluation

	Pile A	Pile B
The First Limit Load (kN)	1,177	687
The Second Limit Load (kN)	1,570	981

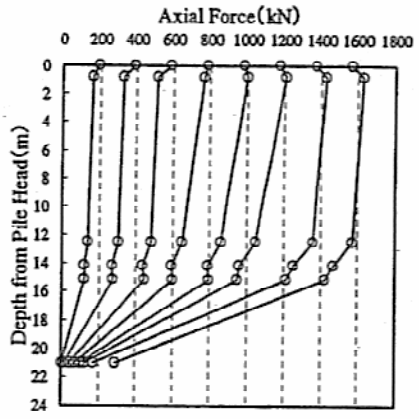

Figure 5. Axial Force Distribution (Pile A)

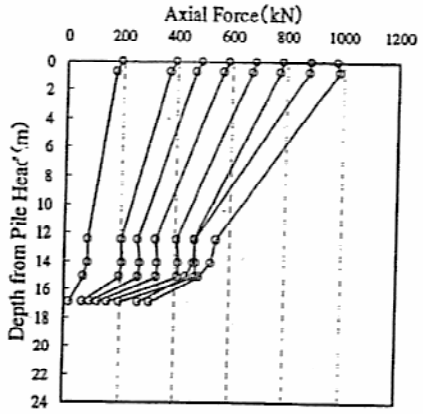

Figure 6. Axial Force Distribution (Pile B)

Table 3. Bearing Capacity Distribution

		Pile A	Pile B
The Second Limit Load		1,570kN	981kN
Skin Friction	Steel Pipe Section	202kN	543kN
	Grout Bond Section	1,192kN	262kN
Toe Resistance		176kN	176kN

Table 4. Comparison of the Skin Friction

	Soil Type	Skin Friction (kN/m^2)
Field Test Data	Fine Sand (N-value 50)	288 (Pile A) 325 (Pile B)
Standard (Ground ancor)	Sand (N-value 50)	294~392

Figure 8 shows the load – displacement curve measured at the pile top during Statnamic load testing of pile A. The maximum load reached 1,930 kN, exceeding the second limit load (1,570 kN) confirmed by the static load testing, a difference assumed to be the result of dynamic effects.

The simple unloading point method was applied to calculate the static resistance that is the measurement data with the dynamic effect removed. Figure 9 shows the pile and soil model for this method. The pile is assumed to be a single mass with a mass M, the non-linear spring K represents the static resistance F_w, the dash pot C represents the ground resistance F_v that is proportional to the velocity v of the pile. The ground resistance F_{soil} is the sum of F_w and F_v.

F_{soil} is obtained by deducting the inertial force F_a from the Statnamic load F_{stn}.

$$F_{soil} = F_{stn} - F_a = F_{stn} - M \cdot a \qquad (1)$$

And F_w is obtained by deducting F_v from F_{soil}.

$$F_w = F_{soil} - F_v = F_{soil} - C \cdot v \qquad (2)$$

Because the velocity v is zero at the point of maximum displacement (unloading point), F_{soil} and F_w are equal at this point. Consequently, the damping constant C is obtained by the following equation. And C is assumed to be constant during loading.

$$C = \{F_{soil\,(max)} - F_{soil\,(v=0)}\} / v^* \qquad (3)$$

Where: v^* is the velocity at the point of maximum F_{soil}.

Figure 10 shows the relationship of the displacement with F_{soil} and F_w obtained using the unloading point method. It also shows the load – displacement curve obtained by static load testing. This figure reveals that F_w increases until the displacement reaches 20 mm, but it declines above this level, then when the displacement reaches 40

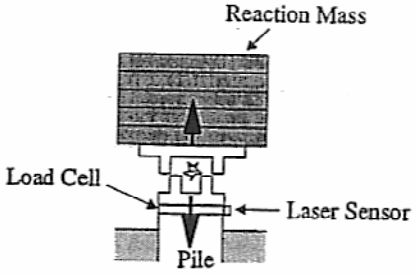

Figure 7. Statnamic Loading Principle

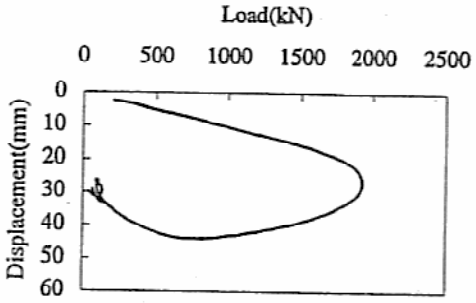

Figure 8. Load-displacement Curve (Statnamic Test Result)

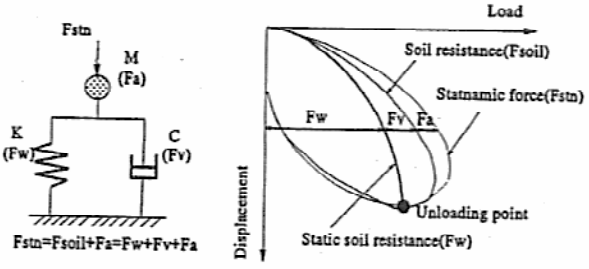

Figure 9. Pile-Soil Model for Unloading Point Method

mm, it rises again: a process that does not reproduce the actual phenomenon. This is assumed to be a result of an over-estimation of the damping constant after the displacement has exceeded 20 mm: a consequence of the assumption that the damping constant C is fixed (540 kN · s/m). Therefore, the precision of the estimation of the static resistance is improved by setting the damping constant based on the skin and the toe and varying it to conform with the state of ground deformation (elastic range or plastic range).

And in a range where the penetration velocity of the pile is small prior to maximum load, even with the unloading point method, it conforms closely to the results of the static load testing. It is, therefore, assumed that it is possible to forecast the spring stiffness of the ground from the initial gradient of the static resistance (F_w) − displacement curve obtained with the unloading point method, that it can be estimated up to the first limit load, and that it can be fully applied as a confirmation test.

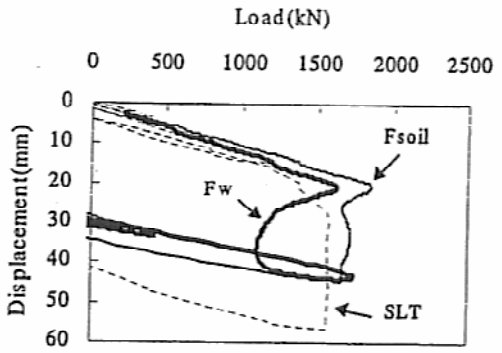

Figure 10. Comparison of the Load–Displacement Relationships from the Static Load Test and the Statnamic Load Test

(3) Applicability of integrity testing

A micropile is constructed so that most of the bearing capacity is provided by the grout bond section and it is extremely important to inject the grout in accordance with the design. It is, however, impossible to directly confirm the shape of the grout from above the ground. For this reason, a study was done of the applicability of integrity testing that can be used to non-destructively estimate the shape of a pile immediately after it is executed.

Integrity testing is usually done by generating low level strain by tapping the top of a pile with a hand held hammer and measuring the response of the pile with an accelerometer. Figure 11 is an example of a measured waveform obtained from an integrity test of an RC pile with a length of 4.0 m and diameter of 300 mm and with the expanded part of its toe. As this figure demonstrates, it is possible to confirm the waves reflected from the toe and the expanded base of a pile made of uniform material and fluctuating section area to estimate the pile length with high precision. But because a micropile has a compound body consisting of steel pipe, grout, and reinforcing steel bars, it is a challenge to set a number of wave propagation velocity. It is assumed that an integrity test of a micropile produces extremely complex waveforms including waves reflected from the joints in the steel pipe and the reinforcing steel bars.

The integrity testing of the micropiles was done after the grout had hardened. The testing was done by installing an accelerometer on the grout at the top of the pile then lightly tapping it with a plastic hammer. The wave propagation velocity was set at 4,250 m/sec that was measured during the Statnamic load testing. Figure 12 shows the velocity waveform at the pile top obtained from testing of pile A. In this figure, velocity is normalized based on the peak value at the pile top and the pile length is estimated by multiplying the measurement time by the propagation velocity. Integrity testing clarifies the reflected waves from the point where the impedance changes, and if the sectional area or the Young's modulus increases, reflected waves are generated in the direction opposite to the input, but if one of these

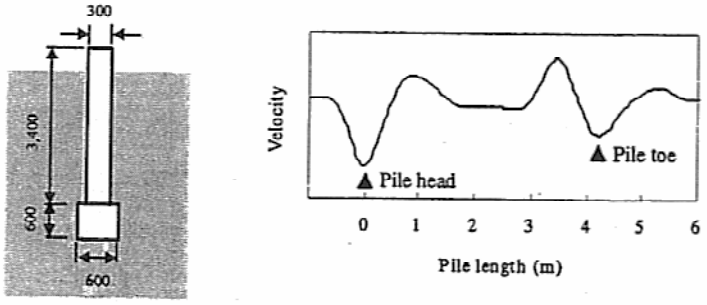

(a)Test Pile (b)Measured Waveform

Figure 11. Shape of Test Pile and Measured Waveform obtained from Integrity Test